Article

Not peer-reviewed version

Formulation and Optimization of a Melissa officinalis Loaded Nanoemulgel for Anti-Inflammatory Therapy Using Design of Experiments (DoE)

Yetukuri Koushik *, Nadendla Rama Rao, Uriti Sri Venkatesh, Gottam Venkata Rami Reddy, Amareswarapu V Surendra, Thalla Sreenu

Posted Date: 9 June 2025

doi: 10.20944/preprints202506.0615.v1

Keywords: Experimental design; nanoemulsion; Melissa officinalis; transdermal system; anti-inflammatory; antimicrobial; controlled drug release; Response Surface Methodology

Article

Formulation and Optimization of a *Melissa officinalis* Loaded Nanoemulgel for Anti-Inflammatory Therapy Using Design of Experiments (DoE)

Yetukuri Koushik [1,*], Nadendla Rama Rao [1], Uriti Sri Venkatesh [2], Gottam Venkata Rami Reddy [1], Amareswarapu V Surendra [3], and Thalla Sreenu [4]

[1] Department of Pharmaceutics, Chalapathi Institute of Pharmaceutical Sciences, Lam, Guntur, Andhra Pradesh and 522034, India

[2] Department of Pharmacology, Sri Sivani College of Pharmacy, Chilakapalem Junction, etcherla, Srikakulam, Andhra Pradesh and 532410, India

[3] Department of Pharmaceutics, KL College of Pharmacy, Koneru Lakshmaiah Education Foundation, Green Fields, Vaddeswaram, Guntur, Andhra Pradesh and 522502 , India

[4] Department of Pharmacology, Vignan Pharmacy College, Vadlamudi, Guntur, Andhra Pradesh and 522213, India

* Correspondence: yetukurikoushik@gmail.com; Tel.: +91 8500008019

Abstract: This research explores the use of a Design of Experiments (DoE) framework for the development and systematic refinement of a nanoemulsion comprising *Melissa officinalis* essential oil for transdermal drug delivery applications. Fourier-transform infrared spectroscopy (FTIR) confirmed the presence of characteristic phytochemical groups such as hydroxyl (–OH), carbonyl (C=O), and ether (C–O–C), pointing to the oil's phytochemical makeup. To examine the effect of various formulation factors, a Central Composite Design (CCD) was implemented. This strategy aimed to minimize droplet size and enhance emulsion stability by evaluating the influence of Tween 80 concentration and homogenization time. The optimized formulation resulted in an average droplet diameter of 127.31 nm, a polydispersity index of 17.7%, 88.3% transmittance, and a zeta potential of –25.0 mV, indicating favorable colloidal stability and uniformity. The drug release study revealed that the release pattern adhered to the Higuchi model ($R^2 = 0.900$; $k = 4.63$), which suggests a diffusion-driven mechanism. Further kinetic analysis based on the Korsmeyer–Peppas equation ($n = 0.88$) indicated a non-Fickian, or anomalous, release behavior. In vitro antimicrobial testing showed that *Staphylococcus aureus* (MIC = 250 µg/mL) was more sensitive to the formulation compared to *Escherichia coli* (MIC = 500 µg/mL). Evaluation of anti-inflammatory efficacy in vivo, using a carrageenan-induced paw edema model, showed that the formulation significantly decreased inflammation ($p = 0.005$ at 60 minutes), with full reduction by 240 minutes. These outcomes highlight the therapeutic value of *Melissa officinalis* oil-based nanoemulgel as a promising carrier for transdermal management of microbial infections and inflammatory conditions.

Keywords: experimental design; nanoemulsion; *Melissa officinalis*; transdermal system; anti-inflammatory; antimicrobial; controlled drug release; response surface methodology

1. Introduction

Human skin, the body's largest organ, performs diverse roles by forming a dynamic boundary between internal physiology and the external surroundings. It acts as a crucial physical, chemical, and immunological defense mechanism. Anatomically, the skin consists of three primary strata—epidermis, dermis, and hypodermis—each of which contributes to maintaining internal equilibrium, defending against microbial invasion, and initiating wound repair mechanisms. However, the skin often faces damage from external insults such as UV radiation, pollutants, and pathogenic

 doi:10.20944/preprints202506.0615.v1

microorganisms, alongside intrinsic contributors like aging and persistent inflammation. These factors collectively lead to increased reactive oxygen species (ROS) production, immune system disturbances, and compromise of the skin's protective function, ultimately playing a role in the onset of inflammatory skin conditions like eczema and psoriasis [1,2]. In recent years, essential oils (EOs) have garnered attention due to their wide-ranging pharmacological effects, such as antimicrobial, anti-inflammatory, and antioxidant actions, attributed to their complex mixture of bioactive molecules like terpenoids and phenolics. *Melissa officinalis* (lemon balm) oil, known for its richness in citral, citronellal, and rosmarinic acid, demonstrates notable activity in modulating oxidative pathways and inflammation-related mechanisms [3].

Despite these benefits, the therapeutic use of essential oils is constrained by limitations such as high volatility, chemical degradation, and limited skin penetration, especially through the stratum corneum the outermost barrier layer. To overcome these issues, nanoscale delivery platforms have been widely investigated for EO encapsulation. Advanced carriers like liposomes, solid lipid nanoparticles (SLNs), nanostructured lipid carriers (NLCs), and nanoemulsions have shown promise due to their ability to improve solubility, enhance stability, and increase bioavailability, thereby enhancing the clinical effectiveness of essential oils [4,5]. Among these systems, nanoemulsions have emerged as promising candidates due to their thermodynamic stability, ease of preparation, and capacity for solubilizing both hydrophilic and lipophilic agents [6]. Low-energy emulsification techniques are often preferred, allowing for the generation of nano-sized droplets (typically ranging from 20 to 200 nm) without subjecting the formulation to elevated temperatures. These techniques support reproducibility, scalability, and cost-effectiveness, making them suitable for both industrial and pharmaceutical use. By incorporating nanoemulsions into a gel base, nanoemulgels are produced, which combine the advantages of both systems providing prolonged retention, improved drug permeation, and enhanced patient compliance [7]. This hybrid system is particularly suitable for localized and sustained drug release in conditions such as skin inflammation.

In this context, the current investigation focused on the formulation and systematic development of a *Melissa officinalis* oil-based nanoemulgel (M-NG). A Central Composite Design (CCD) under the Quality by Design (QbD) paradigm was implemented to evaluate the impact of formulation variables, including surfactant and oil concentrations, on critical quality attributes such as droplet size, zeta potential, and polydispersity index. The optimized nanoemulgel was further assessed for physicochemical characteristics, release kinetics, antimicrobial performance, and anti-inflammatory efficacy using a carrageenan-induced rat paw edema model.

2. Results and Discussion

2.1. FT-IR Analysis of Melissa Oil

The infrared spectrum of Melissa oil shows multiple functional moieties typical of essential oils, underscoring its rich phytochemical content. Spectra were acquired on a Bruker ALPHA II instrument fitted with an ATR module. Measurements covered 4000–400 cm^{-1} at 4 cm^{-1} resolution, with 32 co-added scans to enhance signal reliability. A broad, intense band at 3821.54–3740.35 cm^{-1} corresponds to O–H stretching of free hydroxyl groups, indicative of alcohols and phenolics. A feature at 3498.79 cm^{-1} suggests hydrogen-bonded O–H vibrations. Pronounced C–H stretching absorptions appear at 2921.97, 2863.12, and 2734.83 cm^{-1}, confirming aliphatic chains—particularly methyl and methylene groups—in the oil.

 doi:10.20944/preprints202506.0615.v1

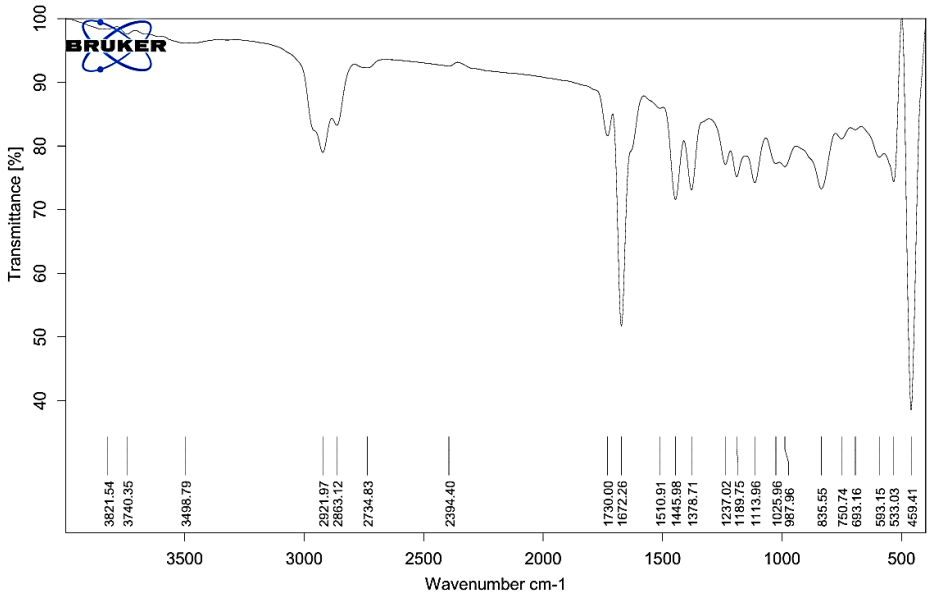

Figure 1. FT-IR spectrum of Melissa oil showing characteristic peaks for functional groups including O–H (3821–3498 cm^{-1}), C–H (2921–2734 cm^{-1}), C=O (1730, 1672 cm^{-1}), C=C and CH bending (1510–1378 cm^{-1}), and C–O (1237–1025 cm^{-1}), confirming the presence of terpenes, esters, alcohols, and phenolic compounds.

A minor peak at 2394.40 cm^{-1} might be attributed to overtones or trace compounds. Strong absorption bands at 1730.00 and 1672.26 cm^{-1} are assigned to C=O stretching, suggesting the presence of esters and ketones, which are common bioactive components in Melissa oil. Peaks at 1510.91, 1445.89, and 1378.71 cm^{-1} further support the presence of C=C (aromatic or alkene) and C–H bending vibrations typical of alkane chains. The C–O stretching region showed significant peaks at 1237.02, 1180.75, 1113.96, and 1025.96 cm^{-1}, indicating ether or alcohol functionalities, while peaks at 987.69 and 925.59 cm^{-1} could be associated with out-of-plane bending of =C–H groups or cyclic terpenes. Distinct absorption in the fingerprint region includes peaks at 835.55, 750.74, 693.16, 593.15, 533.13, and 459.41 cm^{-1}, contributing to the unique identity of Melissa oil. These observations confirm the presence of essential oil constituents such as terpenes, esters, alcohols, and phenolics, which support the oil's traditional therapeutic applications. The functional groups identified from the recorded absorption bands are detailed in Table 1, which lists the standard wavenumber intervals associated with each group. These spectral results affirm the existence of bioactive constituents such as monoterpenes, sesquiterpenes, esters, alcohols, and phenolic derivatives, thereby confirming the phytochemical composition of Melissa oil and reinforcing its suitability for use in both therapeutic and cosmeceutical product development.

Table 1. Characteristic FTIR Bands of Melissa Oil and Corresponding Functional Groups.

Observed Wavenumber (cm^{-1})	Assigned Functional Group	Typical wavenumber Range (cm^{-1})	Presumed Compound Class
3821.54, 3740.35	O–H stretch	3200–3700	Alcohols, Phenols
3498.79	H-bonded O–H stretch	3200–3600	Phenolics, Hydroxyl groups
2921.97, 2863.12, 2734.83	C–H stretch	2800–3000	Alkanes (saturated hydrocarbons)

 doi:10.20944/preprints202506.0615.v1

1730.00, 1672.26	C=O stretch	1650–1750	Esters, Ketones
1510.91, 1445.89, 1378.71	C=C stretch, CH bend	1350–1600	Aromatics, Alkanes, Alkenes
1237.02, 1180.75, 1113.96, 1025.96	C–O stretch	1000–1300	Alcohols, Ethers
987.69, 925.59	=C–H bending	800–1000	Terpenes, Aromatics
835.55, 750.74, 693.16	C–H out-of-plane bend	650–900	Aromatic or cyclic compounds
593.15, 533.13, 459.41	Fingerprint region	<600	Specific spectral features

2.3. Preparation and Optimization of MelissaNanoemulsions

Melissa-oil nanoemulsions were optimized through a statistical response-surface design, with droplet diameter and zeta potential serving as key quality parameters. The experimental matrix listed both real and coded settings for two process factors: the surfactant level (Tween 80, X_1) and the duration of homogenization (X_2). The objective was to obtain the smallest possible droplets while preserving electrokinetic stability. Results showed that both factors significantly affected droplet size. The minimum diameter (110.98 nm) occurred when Tween 80 was at its midpoint ($X_1 = 0$) and homogenization time was at the upper axial value (X_2 = A, 34.14 min), implying that prolonged high-shear processing narrows the size distribution. Conversely, the largest droplets (201.1 nm) formed when both variables were at their lowest settings ($X_1 = -$, $X_2 = -$), reflecting inadequate surfactant content and mechanical energy for effective emulsification.

Table 2. Experimental Design Matrix with actual and coded levels of variables, and Observed Particle Size and Zeta Potential.

Formulations	X_1 (Coded Level)	X_2 (Coded Level)	Tween 80 (%) X_1	Homogenization time (min) X_2	Particle Size (nm)	Zetapotential
1	0	0	4	20	147.7	-25
2	0	0	4	20	129.5	-24.9
3	−	−	2	10	201.1	-12.8
4	0	0	4	20	132.9	-25.4
5	0	A	4	34.1421	110.98	-25
6	0	0	4	20	140.8	-24.1
7	+	+	6	30	119.1	-28.7
8	−	+	2	30	150.6	-21.8
9	a	0	1.17157	20	160.28	-15.9
10	+	−	6	10	181.34	-22.8
11	0	0	4	20	139.67	-23.7
12	A	0	6.82843	20	132.89	-25.1
13	0	a	4	5.85786	173.52	-15.8

Excess Tween 80 (X1 = A or +) did not yield substantial improvements in droplet size reduction, implying the presence of a saturation point beyond which emulsification efficiency plateaus. Similarly, higher homogenization times continued to benefit particle size reduction up to a certain threshold. The optimal formulation was characterized by moderate Tween 80 (4%) and extended homogenization (34.14 min), striking a balance between emulsifier availability and mechanical energy. Following regression analysis using Design Expert (Version 13) software, a polynomial

 doi:10.20944/preprints202506.0615.v1

model incorporating squared terms was generated to describe the influence of formulation factors on particle size:

$$PZ = 143.92 - 23.56X1 - 27.89X2 + 1.89X1X2 + 9.63X1^2 + 5.74X2^2$$

where *PZ* represents particle size (nm), *X1* denotes Tween 80 concentration (coded values for 2–6%), and *X2* refers to homogenization time (coded values for 10–30 min). The model indicates that both Tween 80 and homogenization time exert a significant negative linear effect on particle size, contributing to size reduction. However, the positive quadratic terms suggest that beyond certain optimal points, further increases may not enhance the formulation performance. The model's statistical validity was supported by ANOVA (Table 3), with an overall p-value of 0.0021, indicating high model significance. Individual terms for Tween 80 ($p = 0.0047$) and homogenization time ($p = 0.0022$) were also highly significant. The quadratic term for Tween 80 ($p = 0.0481$) was marginally significant, suggesting a non-linear influence. In contrast, the interaction between Tween 80 and homogenization time was not significant ($p = 0.7442$), indicating that the two factors function independently in their effects on particle size.

Table 3. Statistical Analysis of Model Parameters Using ANOVA.

Factor	df	Overall Variability	Mean Square	F-Statistic	p-Value	Statistical Significance
Model	5	6564.29	1312.86	12.47	0.0021	Significant
Error	7	736.71	105.24	–	–	–
Total	12	7301	–	–	–	–
Intercept	–	–	143.92	28.72	<0.0001	Highly significant
Tween 80	1	–	−23.56	−4.11	0.0047	Highly significant
Homogenization Time	1	–	−27.89	−5.24	0.0022	Highly significant
Tween 80 × Homogenization Time	1	–	1.89	0.34	0.7442	Not significant
Tween 80 × Tween 80	1	–	9.63	2.71	0.0481	Marginally significant
Homogenization Time × Time	1	–	5.74	1.28	0.2417	Not significant
R^2	–	0.8992	–	–	–	Indicates strong model fit
Adjusted R^2	–	0.8465	–	–	–	Adjusted for predictors

The model exhibited a coefficient of determination (R^2) of 0.8992, demonstrating that 89.92% of the variability in particle size can be explained by the model. The adjusted R^2 of 0.8465 confirms the model's reliability after considering for the number of predictors.

The contour plots illustrate the combined influence of Tween 80 percentage (X1) and homogenization time (X2) on the physicochemical characteristics of Melissa oil nanoemulsions, specifically particle size and zeta potential (Figure 2). The particle size contour plot (A) reveals a pronounced decrease in particle size with increasing Tween 80 concentration from 2% to 6% and prolonged homogenization time from 10 to 30 minutes, achieving a minimum size near 110.98 nm. This reduction is attributed to enhanced surfactant-mediated interfacial tension reduction and increased mechanical shear, facilitating effective droplet disruption and stabilization. The zeta potential contour plot (B) demonstrates that higher Tween 80 concentrations and extended

 doi:10.20944/preprints202506.0615.v1

homogenization times result in increasingly negative zeta potential values, reaching approximately –28.7 mV. The elevated negative surface charge promotes electrostatic repulsion between dispersed droplets, thereby enhancing colloidal stability by preventing coalescence and aggregation. Collectively, these contour plots substantiate that optimizing both surfactant concentration and homogenization duration is critical for producing stable Melissa oil nanoemulsions with reduced particle size and enhanced surface charge, which are essential parameters for improved formulation performance and shelf-life stability.

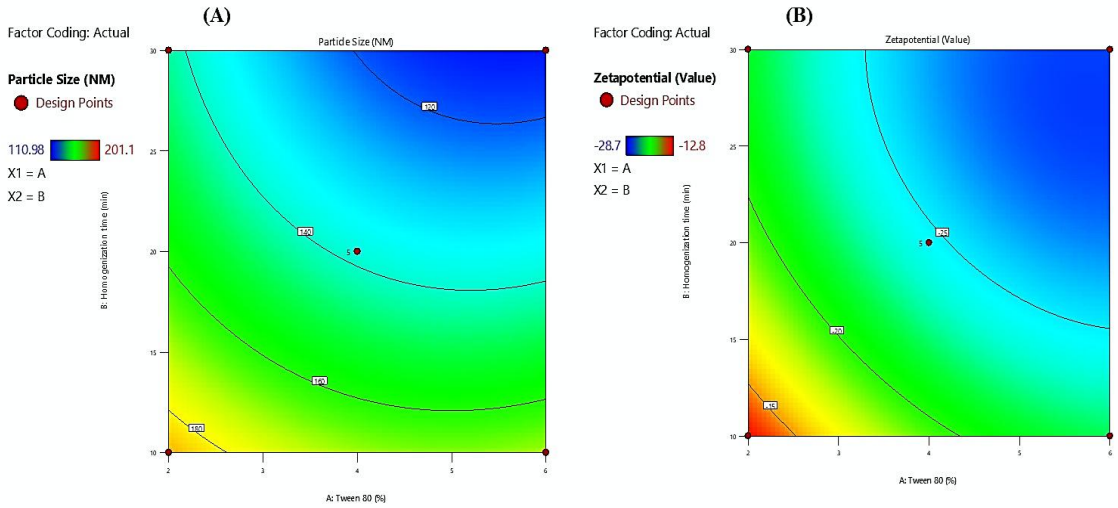

Figure 2. Contour plots depicting the interactive impact of Tween 80 (%) and homogenization time (minutes) on (A) particle size (nm) and (B) zeta potential (mV) of Melissa oil nanoemulsions. The plots demonstrate that increasing Tween 80 concentration and homogenization time significantly reduces particle size and enhances the negative surface charge, indicating improved nanoemulsion stability.

The 3D surface plots presented illustrate the influence of Tween 80 concentration (X1) and homogenization time (X2) on the particle size and zeta potential of Melissa oil nanoemulsion (Figure 3). In the first plot (A), particle size is significantly affected by both variables. As the concentration of Tween 80 increases from 2% to 6% and the homogenization time extends from 10 to 30 minutes, a reduction in particle size is observed. The smallest particle size achieved is around 110.98 nm, indicating improved emulsification efficiency at higher surfactant levels and prolonged homogenization, likely due to enhanced shear force and better droplet breakup. In the second plot (B), zeta potential values become more negative with increasing Tween 80 concentration and homogenization time, reaching a value of 28.7 mV. This trend signifies enhanced physical stability of the nanoemulsion, as higher negative zeta potential values indicate stronger electrostatic repulsion between droplets, preventing aggregation. Overall, these plots confirm that optimal formulation parameters higher Tween 80 concentration and adequate homogenization time are critical for achieving stable nanoemulsions with small particle sizes and improved surface charge stability.

 doi:10.20944/preprints202506.0615.v1

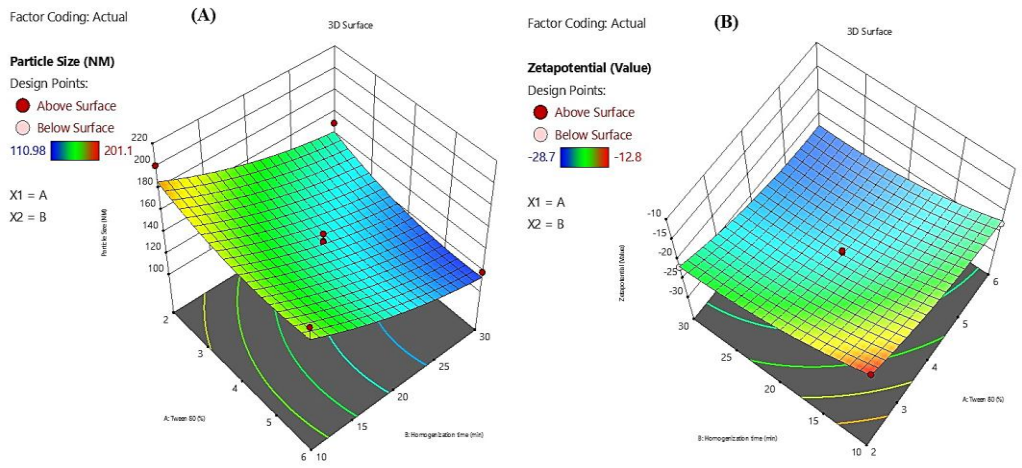

Figure 3. 3D surface plots illustrating the combined effects of Tween 80 concentration (X1) and homogenization time (X2) on (A) particle size and (B) zeta potential of Melissa oil nanoemulsion. The plots demonstrate that increasing Tween 80 concentration and homogenization time leads to a significant decrease in particle size and a more negative zeta potential, indicating enhanced emulsification efficiency and improved nanoemulsion stability.

The overlay plot illustrates the optimized formulation space for minimizing particle size in the Melissa oil nanoemulsion by adjusting Tween 80 concentration (X1) and homogenization time (X2) (Figure 4). The highlighted yellow area represents the design space where the particle size meets the desired minimum criteria, approximately 114 nm. Red points mark the experimental design runs, with the central point indicating the optimal condition of 5.6% Tween 80 and 30 minutes homogenization time. This plot emphasizes the synergistic effect of surfactant concentration and homogenization duration on reducing particle size, which is critical for achieving enhanced stability and efficacy of the nanoemulsion. The overlay visualization aids in clearly defining the optimal parameters for formulation development.

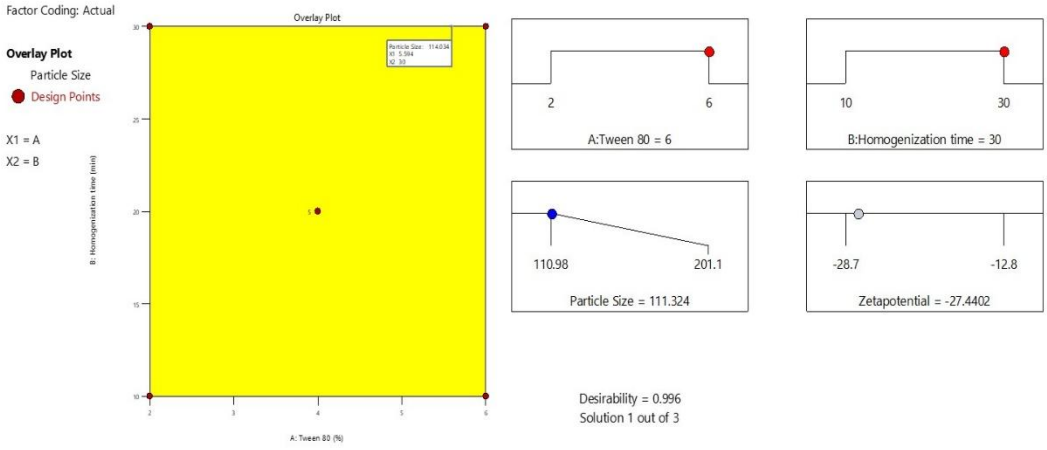

Figure 4. Overlay plot depicting the optimal design space for particle size reduction in Melissa oil nanoemulsion. The yellow region indicates the interaction between Tween 80 concentration (%) and homogenization time (minutes) that results in minimized particle size (114 nm). Red dots represent experimental design points, with the central point marking the optimum formulation conditions.

 doi:10.20944/preprints202506.0615.v1

2.3. Characterization Study of Melissa-Loaded Nanoemulsions (M-NE)

To identify a formulation with optimal performance, freshly developed Melissa oil nanoemulsions (M-NEs) were subjected to a series of characterization and stability assessments. Over a 60-day observation period under varying thermal storage conditions, the formulations demonstrated excellent physical stability, with no visible signs of creaming, phase separation, or noticeable alterations in color or transparency. Furthermore, thermodynamic stability was verified through successive heating-cooling and freeze-thaw cycles, indicating the formulation's resilience against temperature-induced stress. Based on the design space predicted through CCD and the associated prediction profiles, the most stable formulation exhibiting the most favorable physicochemical attributes was selected for subsequent investigations.

2.4. Physicochemical Characteristics and Morphological Analysis

The particle size analysis of the Melissa oil nanoemulsion revealed a hydrodynamic diameter of 127.31 nm with a polydispersity index (PDI) of 17.7%, indicating a moderately uniform distribution and stable dispersion. The transmittance value of 88.3% further supports the clarity and homogeneity of the formulation. Zeta potential measurements exhibited a value of −25.0 mV, suggesting good colloidal stability by ensuring sufficient electrostatic repulsion between particles, thereby preventing aggregation. The standard deviation of 0.7 mV and a distribution peak at −23.5 mV confirm the consistency of the surface charge across the sample. Overall, these findings indicate that the Melissa oil nanoemulsion possesses suitable physicochemical properties for potential transdermal or topical application, offering stable droplet distribution and robust colloidal stability (Figure 5).

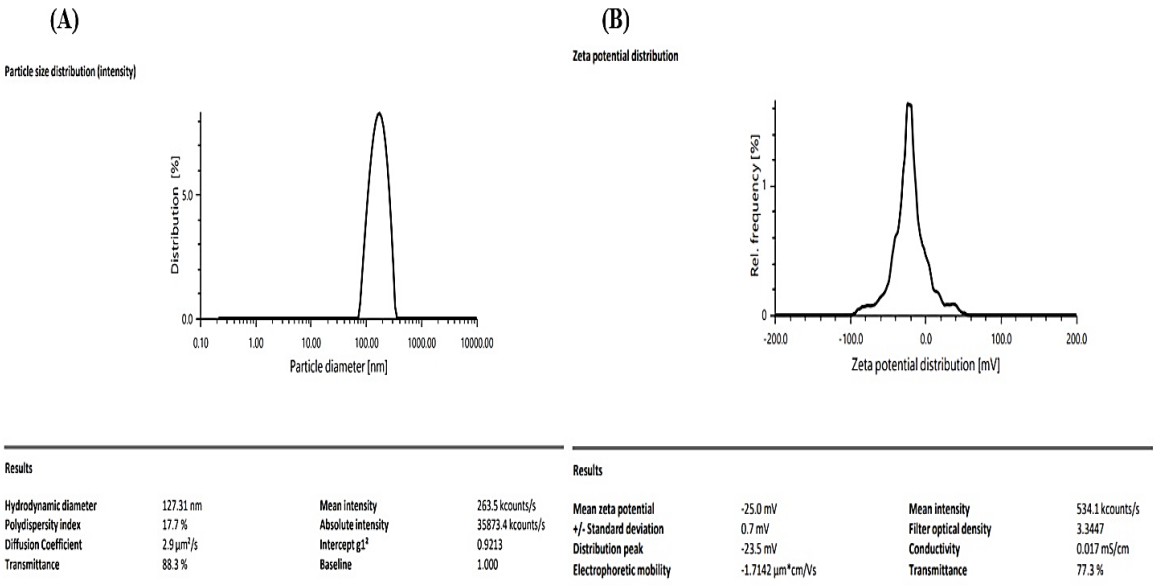

Figure 5. (A) Distribution of Particle sizes in the Melissa nanoemulsion exhibiting uniformity. (B) Zeta potential measurements indicating stable colloidal dispersion.

2.5. Entrapment Efficiency of Melissa Nanoemulsion

A calibration curve for Melissa oil was established over a concentration range of 1 to 15 µg/mL, showing excellent linearity with a correlation coefficient (R^2) of 0.998, indicating the reliability and accuracy of the method. The limit of detection (LOD) and limit of quantification (LOQ) were calculated as 0.46 µg/mL and 1.44 µg/mL, respectively, confirming the sensitivity of the analytical procedure. The Melissa oil content in the optimized nanoemulsion formulation was initially found to

 doi:10.20944/preprints202506.0615.v1

be 97.85 ± 0.38% on the day of preparation. After 60 days of storage under controlled conditions, the content reduced to 91.72 ± 1.22%, corresponding to a retention rate of 93.74%, which reflects the formulation's favorable stability profile over time. The high entrapment efficiency (EE%) of 95.63 ± 0.47% observed in the optimized M-NE formulation suggests that the chosen emulsifier system effectively stabilized the oil droplets and minimized drug leakage, thereby ensuring efficient encapsulation and prolonged retention.

2.6. Design and Evaluation of a Melissa Nanoemulgel (M-NG)

The optimized *Melissa* nanoemulsion (M-NE) was effectively integrated into a hydrogel base to create Melissa nanoemulgel (M-NG), aiming to improve the formulation's suitability for topical use. The base hydrogel was prepared with polyacrylic acid (Carbopol 940), dispersed in distilled water under continuous mixing. The mixture was then neutralized with triethanolamine to achieve a clear gel. Of the tested formulations, the hydrogel containing 1% w/w polyacrylic acid showed ideal physicochemical characteristics such as uniformity, transparency, stable appearance, and good adhesive qualities, as confirmed through the Thumb Test over a 30-day period. Thermal stability evaluation under accelerated storage conditions indicated that the M-NG retained structural integrity without visible evidence of separation, layering, or water release. Formulations with higher polymer concentrations resulted in increased viscosity and enhanced mechanical strength, which aided in maintaining stability during centrifugation; however, they exhibited somewhat lower spreadability, which may influence how easily they can be applied. The optimized M-NG formulation displayed a stable pH of 5.68 ± 0.07 over 30 days of storage, confirming skin compatibility and minimal potential for irritation. Assessments of appearance, consistency, and ease of application using the glass plate method and visual checks validated the consistency and strength of the formulation. These results highlight the promise of the *Melissa* nanoemulgel as a reliable and efficient carrier for skin-based therapeutic use.

2.7. In Vitro Evaluation of Drug Release and Diffusion Profiles

The rate and extent of drug release are vital parameters in assessing the effectiveness of topical formulations. To examine the release profile of Melissa oil from different formulations, a dialysis membrane method was employed over a period of 6 hours (360 minutes). The study compared four distinct formulations: Melissa Nanoemulgel (M-NG), Melissa Nanoemulsion (M-NE), Melissa Nanoemulsion in Carbopol hydrogel base (n-EnM), and Melissa-loaded Hydrogel (n-EnM Hydrogel). The cumulative drug release (%) was measured at intervals of 30 minutes, and the mean values with standard deviations were recorded (Figure 9). At 30 minutes, M-NG demonstrated a drug release of 7.9 ± 1.1%, while M-NE showed 12.2 ± 1.6%, n-EnM released 5.5 ± 1.2%, and n-EnM Hydrogel had a release of 3.0 ± 0.7%. As time progressed, all formulations exhibited sustained release profiles. After 180 minutes, the drug release from M-NG reached 44.5 ± 3.1%, while M-NE released 63.4 ± 3.6%, n-EnM showed 31.2 ± 2.7%, and n-EnM Hydrogel recorded 18.1 ± 1.9%. A gradual increase was observed until the final time point at 360 minutes, where the cumulative release for M-NG was 66.4 ± 4.6%, slightly lower than M-NE (87.5 ± 4.9%), but higher than n-EnM (46.3 ± 3.9%) and n-EnM Hydrogel (27.6 ± 2.6%). These findings highlight the superior release potential of the nanoemulsion system, with the hydrogel matrix further modulating the release pattern. Among the tested systems, M-NE exhibited the highest release percentage, likely due to its smaller droplet size and absence of a gel matrix that might hinder diffusion. However, M-NG presented a more controlled and steady release, suggesting its suitability for sustained therapeutic action through topical delivery.

 doi:10.20944/preprints202506.0615.v1

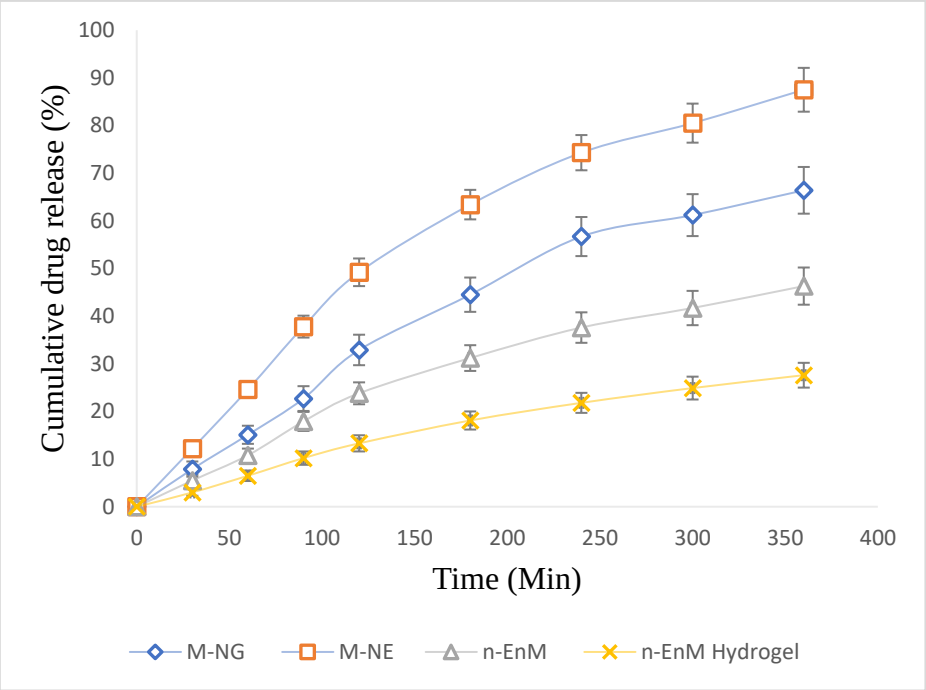

Figure 6. Percentage of cumulative drug release from various Melissa oil formulations over time, expressed as mean ± standard deviation (n = 3). The release curves for M-NG (♦), M-NE (▲), n-EnM (■), and n-EnM Hydrogel (●) illustrate variations in drug release kinetics between the different formulations. Error bars represent standard deviation, indicating the extent of variability in the release patterns.

2.8. Assessment of Antibacterial Efficacy

The antibacterial efficacy of Melissa Nanoemulgel (M-NG) was evaluated against *Staphylococcus aureus* and *Escherichia coli* through the broth dilution technique to establish the minimum inhibitory concentration (MIC). The results revealed that *S. aureus*, a Gram-positive bacterium, was more sensitive to M-NG, with an MIC of 250 µg/mL, while *E. coli*, a Gram-negative bacterium, exhibited reduced susceptibility, showing an MIC of 500 µg/mL. These findings suggest a stronger inhibitory effect of the formulation against Gram-positive pathogens, which may be attributed to differences in cell wall structure and permeability. Although the MIC values of M-NG were higher than those of conventional antibiotics, Melissa oil has a well documented safety profile and is known for its broad-spectrum antimicrobial activity without significant toxicity at therapeutic concentrations. The formulation's suitability for topical application allows for localized delivery at effective concentrations, minimizing systemic exposure. This makes M-NG a promising option for managing microbial infections on the skin, particularly in conditions such as acne, minor wounds, and burns where bacterial colonization is a concern. Furthermore, the dual action of Melissa oil antibacterial and anti-inflammatory may support wound healing and enhance the formulation's therapeutic utility in dermatological care.

2.9. Examination of Dermal Effects in the Acute Irritation Study

The acute skin irritation potential of the Melissa Nanoemulgel (M-NG) formulation was evaluated following OECD Guideline 404, using three groups of healthy male Wistar rats (n = 3 per group). The study aimed to evaluate any observable skin reactions following a single dose application of M-NG. The treated area was observed at 1, 24, 48, and 72 hours post-application, and the severity of dermal responses was scored using a standard irritation scale. At the 1-hour mark, the M-NG group showed slight erythema (median score: **0.5 ± 0.5**), which completely resolved by the 24-hour observation point. No edema or other visible irritation symptoms were recorded at any time point. In comparison, the positive control group (treated with Formalin) exhibited notable erythema and mild edema (median score: **2.5 ± 0.5** at 1 hour), with signs of irritation persisting through 72 hours,

 doi:10.20944/preprints202506.0615.v1

although gradually diminishing in intensity. The negative control group (treated with Blank Gel) displayed no erythema or edema throughout the observation period. Statistical analysis using the **Kruskal-Wallis test** demonstrated a **significant difference ($p < 0.05$)** between the test groups at all time points, particularly between the M-NG and Formalin groups. These results confirm that M-NG causes negligible dermal irritation, comparable to the blank control, and is significantly less irritating than the positive control. This supports its safety and compatibility for topical application, indicating potential for dermatological use without risk of adverse local skin reactions.

Table 3. Acute Dermal Irritation Scores of different groups.

Time Point	Melissa Nanoemulgel [1]	Positive Control (Formalin) [1]	Negative Control (Blank Gel) [1]	p-value [2]
1 hour	0.5 ± 0.5	2.5 ± 0.5	0.0 ± 0.0	0.0274
24 hours	0.0 ± 0.0	2.0 ± 0.5	0.0 ± 0.0	0.0196
48 hours	0.0 ± 0.0	1.5 ± 0.5	0.0 ± 0.0	0.0221
72 hours	0.0 ± 0.0	1.0 ± 0.0	0.0 ± 0.0	0.0303

[1] n = 3 (expressed as median ± interquartile range); [2] $p < 0.05$, indicating a statistically significant difference between groups (Kruskal-Wallis test).

2.10. In-Vivo Assessment of Anti-Inflammatory Activity

The anti-inflammatory activity of the Melissa Nanoemulgel (M-NG) was evaluated using the carrageenan-induced paw edema model in Wistar rats. The study compared three groups: a test group treated with M-NG, a standard group treated with a marketed Diclofenac gel (2.5% w/w), and a control group receiving blank nanoemulgel. Paw swelling was induced via subplantar injection of carrageenan, and the changes in paw volume were measured at 0, 30, 60, 120, 240, and 360 minutes using a plethysmometer. The percent inhibition of edema was calculated at each time point. At 30 minutes post-induction, the M-NG group showed a reduction in paw volume to 0.25 ± 0.006 mL, compared to 0.32 ± 0.005 mL in the standard group and 0.42 ± 0.007 mL in the control. The edema inhibition was 40.5% for M-NG and 23.8% for the standard group. Statistically significant differences were observed between the M-NG and control groups ($p = 0.029$). At 60 minutes, M-NG exhibited 60.3% inhibition (volume: 0.17 ± 0.004 mL) compared to 33.2% in the standard group (0.28 ± 0.005 mL), with a highly significant difference ($p = 0.008$). At 120 minutes, M-NG further reduced paw volume to 0.07 ± 0.003 mL (81.6% inhibition), while the standard maintained a moderate effect (0.19 ± 0.004 mL, 52.6% inhibition). Although the M-NG group consistently outperformed the standard, the difference did not reach statistical significance at this time point ($p = 0.076$). At 240 minutes, inflammation in the M-NG group was nearly eliminated (0.01 ± 0.001 mL, 96.9% inhibition), compared to the standard group (0.05 ± 0.001 mL, 86.5% inhibition). At 360 minutes, complete resolution of edema was observed in both M-NG and standard groups (100% inhibition), while the control group still showed residual swelling (0.33 ± 0.002 mL). These findings confirm the superior anti-inflammatory potential of Melissa Nanoemulgel over the standard treatment. The formulation demonstrated rapid onset, sustained effect, and complete resolution of inflammation without adverse effects, establishing its promise for topical management of inflammatory skin conditions.

Table 4. *In-Vivo* Evaluation of Anti-Inflammatory Activity: Edema Reduction and Statistical Analysis.

Time (min)	Negative Control Group (mL)[1]	Positive Control Group (mL) [1]	Treatment Group (mL) [1]	Inhibition of Edema (%)	Group Comparisons	Mean Difference (mL)	p-value[4]

 doi:10.20944/preprints202506.0615.v1

0	0.00 ± 0.00	0.00 ± 0.00	0.00 ± 0.00	-	-	-	-
30	0.42 ± 0.007	0.32 ± 0.005	0.25 ± 0.006	23.8 [2] / 40.5 [3]	Negative Control vs. Standard	-0.17	0.029
60	0.41 ± 0.006	0.28 ± 0.005	0.17 ± 0.004	33.2 [2] / 60.3 [3]	Negative Control vs. Treatment	-0.24	0.008
120	0.39 ± 0.005	0.19 ± 0.004	0.07 ± 0.003	52.6 [2] / 81.6 [3]	Standard vs. Treatment	-0.12	0.076
240	0.36 ± 0.003	0.05 ± 0.001	0.01 ± 0.001	86.5 [2] / 96.9 [3]	-	-	-
360	0.33 ± 0.002	0.00 ± 0.00	0.00 ± 0.00	100 [2,3]	-	-	-

[1] Mean ± Standard Error of the Mean (n = 6); [2] Percentage inhibition calculated in comparison with the Positive Control Group (Standard, S). [3] Percentage inhibition calculated relative to the Treatment Group (T). [4] A p-value less than 0.05 was considered statistically significant.

3. Conclusion

The *Melissa officinalis* oil-based nanoemulgel was successfully developed and optimized using a Quality by Design (QbD) strategy, focusing on Tween 80 concentration and homogenization time as key formulation variables. FTIR spectroscopy confirmed the presence of functionally active bio-compounds, supporting the medicinal potential of Melissa oil. The optimized formulation exhibited desirable physicochemical properties, including a droplet size of 127.31 nm, a polydispersity index (PDI) of 17.7%, a zeta potential of −25.0 mV, and light transmittance of 88.3%, indicating that the nanoemulsion was stable, homogenous, and appropriate for transdermal delivery. Drug release studies conducted *in vitro* demonstrated that the release pattern best fit the Higuchi model (R^2 = 0.990), indicating diffusion-dominated behavior. Additionally, results from the Korsmeyer–Peppas model (n = 0.88) suggested that the release followed a non-Fickian, or anomalous, transport mechanism. Antibacterial evaluations showed effective suppression of microbial growth, particularly against *Staphylococcus aureus* and *Escherichia coli*, with *S. aureus* displaying a lower minimum inhibitory concentration (MIC), suggesting greater susceptibility. The anti-inflammatory efficacy of the formulation was further supported by *in vivo* studies, which showed a statistically significant reduction in paw edema (p = 0.005 at 60 minutes) and nearly full resolution by 240 minutes. Overall, these findings support the potential of Melissa oil nanoemulgel as a novel transdermal delivery platform with dual anti-inflammatory and antimicrobial properties suitable for skin-related therapeutic applications.

4. Materials and Methods

4.1. Materials

Melissa essential oil was obtained from Avi Naturals, Delhi, India. Additional components of the formulation, such as Carbopol 934, benzyl alcohol, and sodium hydroxide (NaOH), were acquired from Loba Chemie Pvt. Ltd., Mumbai. The bacterial strains used for microbiological testing

 doi:10.20944/preprints202506.0615.v1

included *Staphylococcus aureus* (MTCC 737) and *Escherichia coli* (MTCC 1035), both of which were provided by the Microbial Type Culture Collection and Gene Bank (MTCC), Chandigarh.

4.2. Surfactant Screening and FT-IR Analysis of Melissa Oil

A structured screening process was conducted to determine the most effective surfactant for developing oil-in-water (O/W) nanoemulsions containing Melissa oil. Various surfactant types were tested, including polysorbates (Tween 80 and Tween 20), sorbitan esters (Span 80 and Span 20), and polyethylene glycol 400 (PEG 400). Each formulation included 5% w/v of Melissa oil, while the concentration of surfactants was varied between 1% and 20% w/v. The evaluation involved parameters such as droplet size, emulsion stability, and clarity to identify the optimal surfactant. Tween 80 emerged as the most suitable candidate, offering the best emulsification capacity, consistent droplet formation, and formulation stability. Consequently, Tween 80 was selected for use in the final formulation [9].

Fourier-transform infrared (FT-IR) spectroscopy of Melissa oil was conducted using an attenuated total reflectance (ATR) accessory (Lab India-Bruker). A small amount of oil was placed directly on the ATR crystal to ensure adequate contact. The spectra were recorded over a range of 4000 to 400 cm^{-1} with a resolution of 4 cm^{-1}, averaging 32 scans to improve precision. Background correction was performed before data acquisition. The obtained spectrum was then examined to identify the characteristic functional groups present in Melissa oil.

4.3. Development and Optimization of Melissa Nanoemulsion

Preliminary formulation work identified that a 5% w/v concentration of *Melissa* essential oil was optimal for developing the nanoemulsion. The nanoemulsion was formulated through an oil-in-water (O/W) emulsification method. During this process, the aqueous phase—consisting of distilled water (89–93% w/v) and Tween 80 (2–6% w/v)—was incrementally added to the oil phase while stirring continuously at 40 °C using a Remi magnetic stirrer for 1 hour to achieve homogeneous mixing. The resulting coarse emulsion was subsequently homogenized at a high shear speed (1400 rpm) for 10 to 30 minutes to produce a stable nanoemulsion system [10].

To systematically optimize the formulation, a Central Composite Design (CCD) approach with two independent variables was implemented using Design Expert Software (Version 13, Stat-Ease Inc.). The variables investigated were surfactant concentration (X_1) and homogenization time (X_2), each evaluated at three levels (2–6% and 10–30 minutes, respectively). The measured responses included droplet size (Y_1), which was aimed to be minimized, and zeta potential (Y_2), which was maintained within an acceptable stability window. Thirteen experimental formulations were created, incorporating one replicate and five center points to ensure statistical reliability. Analysis of variance (ANOVA) was carried out at a 95% confidence interval, applying a statistical significance threshold of $p \leq 0.05$. The formulation demonstrating optimal results i.e., minimum droplet size and desirable zeta potential—was selected for detailed evaluation and characterization.

4.4. Assessment of Entrapment Efficiency

The entrapment efficiency (EE) of the Melissa oil nanoemulsion (M-NE) was determined using a modified UV-visible spectrophotometric procedure, adapted from previously published methods [11]. A standard calibration curve for Melissa oil was constructed based on the maximum absorbance wavelength (λmax), and the linearity of the curve was verified through regression analysis. Furthermore, the method's sensitivity was established by determining the limit of detection (LOD) and limit of quantification (LOQ), ensuring accuracy and reliability of the results [12]. For the assay, 100 µL of the Melissa nanoemulsion was diluted in a 1:1 (v/v) ethanol and distilled water solution. UV-Vis spectroscopy was then employed to quantify the amount of Melissa oil present in each sample. Blank formulations without the essential oil were used to eliminate background interference. All measurements were performed in triplicate to improve accuracy and reproducibility.

 doi:10.20944/preprints202506.0615.v1

4.5. Physicochemical Characterization and Stability Assessment

The Melissa oil nanoemulsions were characterized for their physicochemical properties, such as particle size, polydispersity index (PDI), and zeta potential, employing the Malvern Zetasizer Nano ZS 90 with photon correlation spectroscopy. Particle size and PDI measurements were carried out at 25 °C using disposable polystyrene cuvettes, while zeta potential was analyzed using omega cuvettes [13]. Stability of the nanoemulsion formulations was assessed through stress testing involving thermal and freeze-thaw cycles. For thermal stress, samples underwent alternating heating and cooling cycles between 40 °C and 48 °C, each cycle lasting 48 hours and repeated three times. Following each cycle, the samples were checked for any signs of phase separation or instability. For freeze-thaw testing, the emulsions were frozen at -20 °C and thawed at room temperature (25 °C) across three cycles. After completion, centrifugation was performed to evaluate physical stability and detect any formulation breakdown [14].

4.6. Preparation of Melissa Oil – Loaded Nanoemulgel

The nanoemulgel comprising Melissa oil (M-NG) was developed using Carbopol 940 as the gelling matrix at concentrations varying between 0.5% and 2% w/w. The gelling agent was slowly incorporated into the pre-formulated Melissa nanoemulsion with continuous agitation to ensure homogeneity. To enhance preservation and maintain product stability, benzyl alcohol was included, and the pH was finely tuned with 1 M sodium hydroxide to ensure suitable skin tolerance. The final formulation was evaluated for physical properties including appearance, clarity, homogeneity, foaming tendency, and leakage. A Thumb Test was used to examine spreadability and adhesion. Spreadability was determined via the glass slide technique, and viscosity was evaluated using a Brookfield viscometer (ULA S00 spindle, 4 rpm, torque at level 10) [16]. pH stability was monitored to evaluate compatibility and long-term storage potential with skin.

4.7. Analysis of In Vitro Drug Diffusion and Kinetic Modeling

The release profile of the Melissa nanoemulgel (M-NG) was analyzed using a modified Franz diffusion cell system [17]. A cellophane membrane with 12 kDa molecular cut-off was pre-soaked in a 1:1 ethanol–water mixture overnight for hydration. About 1 gram of M-NG was positioned in the donor compartment. At regular time intervals, samples were collected from the receptor chamber, replacing it with an equal amount of fresh medium each time to ensure sink conditions. The system was maintained at 32 °C with continuous stirring at 200 rpm throughout the experiment [18]. The samples were diluted and analyzed using UV-spectrophotometry at the maximum absorbance of Melissa oil. A previously constructed standard curve was used for quantification. A placebo formulation (without Melissa oil) served as a blank to prevent any interference from excipients. Additionally, the release pattern of a nanoemulsion formulation without Carbopol (M-NE), free Melissa oil solution, and a conventional hydrogel with Melissa oil in 1% Carbopol 940 were also evaluated for comparison. The findings were reported as mean ± SD from three replicates. The release data were fitted into different kinetic models such as zero-order, first-order, Higuchi, Hixson–Crowell, and Korsmeyer–Peppas to determine the release mechanism [19]. The model with the highest R^2 value was used to determine the most accurate release mechanism.

4.8. Assessment of Antibacterial Potential of M-NG Formulation

The antimicrobial efficacy of the Melissa nanoemulgel (M-NG) was assessed against Staphylococcus aureus (MTCC 737) and Escherichia coli (MTCC 1035) using the broth microdilution assay, conducted in accordance with the CLSI (Clinical and Laboratory Standards Institute) guidelines [20]. A series of two-fold serial dilutions of the M-NG were prepared in Mueller–Hinton Broth (MHB) using a 96-well sterile microtiter plate, with concentrations ranging from 500 µg/mL to 1.95 µg/mL. Fresh cultures of the test organisms were grown on Nutrient Agar and adjusted to a 0.5 McFarland turbidity standard (~1.5 × 10^8 CFU/mL) by suspending them in sterile saline. This

 doi:10.20944/preprints202506.0615.v1

suspension was then appropriately diluted to achieve a final bacterial load of approximately 0.5×10^5 CFU/mL per well, and 100 µL of this bacterial suspension was added into each well. The microplates were incubated at 37 °C for 24 hours under sterile conditions. Bacterial growth was evaluated spectrophotometrically by measuring optical density at 600 nm (OD600) [21]. The Minimum Inhibitory Concentration (MIC) was determined as the lowest concentration of M-NG that completely inhibited visible bacterial growth and showed an OD ≤ 0.1. To validate the assay, three types of controls were used: a sterility control (MHB only), a growth control (bacteria without the test formulation), and a positive control containing ciprofloxacin (2 µg/mL). All experiments were conducted in triplicate, and the findings were reported as mean ± standard deviation (SD) to ensure accuracy and reproducibility.

4.9. Preclinical Evaluation Using Animal Models

The in vivo study was conducted using male Wistar rats (body weight: 250 ± 10 g). The animals were housed in a controlled environment with temperature maintained at 25 ± 2 °C, a 12-hour light/dark cycle, and unrestricted access to pellet feed and clean drinking water [22]. All experiments adhered to ethical norms specified by the Committee for the Purpose of Control and Supervision of Experiments on Animals (CPCSEA) [28] and were carried out only after receiving approval from the Institutional Animal Ethics Committee (IAEC) under protocol number 07/IAEC/CLPT/2023-24 (Reg. No: 1048/PO/Re/S/07/CPCSEA). The study design ensured animal welfare and ethical compliance throughout the experimental timeline.

4.10. Evaluation of Skin Irritation Following Topical Application

The potential for skin irritation by the Melissa nanoemulgel (M-NG) was assessed following the OECD guideline 404 [23] using healthy male Wistar rats. An amount of 0.5 g of M-NG was applied on a 6 cm^2 shaved skin area and covered with a semi-occlusive dressing for 4 hours. As a control, 0.8% formalin solution served as a positive control, while a blank gel served as the negative control. Following exposure, the area was cleaned with warm water, and observations were made for skin reactions such as redness (erythema) and swelling (edema) at 1, 24, 48, and 72 hours post-treatment.

4.11. Investigation of Anti-Inflammatory Efficacy in Animal Models

The anti-inflammatory effect of M-NG was studied using the carrageenan-induced paw edema model in Wistar rats (n = 6 per group, weight range: 200–300 g). The animals were kept in standardized laboratory conditions (temperature 25 ± 2 °C, 12-hour light/dark cycle) with unlimited access to food and water [24]. This study was approved by the Institutional Animal Ethics Committee (IAEC).

Rats were randomly allocated into three groups: Group 1 received a blank nanoemulgel as a negative control; Group 2 was treated with Dicloran® gel (2.5%) serving as the positive control; and Group 3 was given the M-NG formulation containing 5% w/w Melissa oil. Inflammation was induced by injecting 0.1 mL of 1% w/v carrageenan suspension into the subplantar region of the right hind paw in all groups. Immediately after induction, 0.5 g of the respective formulations was applied topically to the affected paw and gently rubbed to ensure even absorption. The treatment was applied once, and paw edema volume was measured at baseline (0 min) and at intervals of 30, 60, 120, 240, and 360 minutes using a digital vernier caliper by an observer blinded to group assignments. The percentage change in paw volume was calculated using the formula:

$$\%\ \boldsymbol{Change\ in\ Hind\ Paw\ Volume} = \left(\frac{\boldsymbol{Mean\ C_n - Mean\ C_i}}{\boldsymbol{Mean\ C_i}}\right) \times \mathbf{100}$$

where Mean C_n is the average paw volume at each time point, and Mean C_i is the baseline paw volume prior to carrageenan injection. The extent of edema inhibition was compared against the control group to determine the anti-inflammatory efficacy of the M-NG [25].

 doi:10.20944/preprints202506.0615.v1

4.12. Statistical Analysis and Interpretation

Data obtained from the experiments were statistically analyzed using Student's *t*-test for comparisons between two groups and one-way analysis of variance (ANOVA) followed by Tukey-Kramer post hoc test for multiple group comparisons. Results from in vitro evaluations were reported as mean ± standard deviation (SD), whereas in vivo data were presented as mean ± standard error of the mean (SEM). A *p*-value of less than 0.05 was considered indicative of statistical significance, thereby confirming the robustness and reproducibility of the experimental outcomes.

Author Contributions: Conceptualization, Y.K.; methodology, Y.K. and N.R.R.; software, Y.K.; validation, Y.K. and V.R.R.G; formal analysis, S.V.U and A.V.S.; investigation, Y.K. and S.T.; resources, Y.K. and R.V; data curation, Y.K. and R.V.; writing—original draft preparation, Y.K.; writing—review and editing, Y.K. and N.R.R.; visualization, Y.K. and V.R.R.G.; supervision, N.R.R.; project administration, Y.K. All authors have read and agreed to the published version of the manuscript.

Funding: This research received no external funding.

Institutional Review Board Statement: The animal study protocol was approved by the Institutional Animal Ethics Committee (IAEC) of Chalapathi Institute of Pharmaceutical Sciences (Reg. No: 1048/PO/Re/S/07/CPCSEA) under certificate number 07/IAEC/CLPT/2023-24. All experimental procedures were conducted in accordance with the guidelines of the Committee for the Control and Supervision of Experiments on Animals (CCSEA).

Informed Consent Statement: Not applicable.

Data Availability Statement: The data generated in this study can be requested from the corresponding author

Acknowledgments: The authors gratefully acknowledge SRM Institute of Science and Technology, Kattankulathur, Chalapathi Institute of Pharmaceutical Sciences, Guntur, and JSS College of Pharmacy, Ooty for providing guidance, laboratory facilities, and equipment to carry out the research work.

Conflicts of Interest: The authors declare no conflicts of interest.

Abbreviations

The following abbreviations are used in this manuscript:

QbD	Quality by Design
NE	Nanoemulsion
NEs	Nanoemulsions
M-NE	Melissa Nanoemulsion
n-EnM	Nanoemulsion in Matrix
n-EnM Hydrogel	Nanoemulsion in Hydrogel
M-NG	Meliss Nanoemulgel
CCD	Central Composite Design
ANOVA	Analysis of Variance
PDI	Polydispersity Index
CI	Confidence Interval
EE	Entrapment Efficiency
LOD	Limit of Detection
LOQ	Limit of Quantification
SEM	Scanning Electron Microscopy
UV	Ultraviolet
O/W	Oil-in-Water
MHB	Mueller-Hinton Broth

 doi:10.20944/preprints202506.0615.v1

MIC	Minimum Inhibitory Concentration
CLSI	Clinical and Laboratory Standards Institute
CFU	Colony-Forming Unit
IAEC	Institutional Animal Ethics Committee

References

1. Rinnerthaler, M., Bischof, J., Streubel, M. K., Trost, A., & Richter, K. (2015). Oxidative stress in aging human skin. *Biomolecules, 5*(2), 545–589. https://doi.org/10.3390/biom5020545
2. D'Orazio, J., Jarrett, S., Amaro-Ortiz, A., & Scott, T. (2013). UV radiation and the skin. *International Journal of Molecular Sciences, 14*(6), 12222–12248. https://doi.org/10.3390/ijms140612222
3. Taherkhani, M., Goudarzi, M., & Bakhshi, A. (2013). Antibacterial activity of *Melissa officinalis* essential oil against clinical isolates of methicillin-resistant *Staphylococcus aureus*. *Iranian Journal of Microbiology, 5*(4), 263–267.
4. Shakeel, F., Baboota, S., Ahuja, A., Ali, J., & Shafiq, S. (2008). Skin permeation mechanism and bioavailability enhancement of celecoxib from transdermally applied nanoemulsion. *Journal of Nanobiotechnology, 6*(1), 8. https://doi.org/10.1186/1477-3155-6-8
5. Kotta, S., Khan, A. W., Pramod, K., Ansari, S. H., Sharma, R. K., & Ali, J. (2016). Exploring scientifically validated herbal nanoformulations for topical delivery: A review. *Current Nanoscience, 12*(2), 174–190. https://doi.org/10.2174/1573413712666151124201141
6. Bhoyar, N., Thube, R., & Saudagar, R. (2021). Formulation and optimization of nanoemulsion-based gel containing eugenol using response surface methodology. *Journal of Drug Delivery and Therapeutics, 11*(1), 183–189. https://doi.org/10.22270/jddt.v11i1.4527
7. Shakeel, F., Haq, N., Alanazi, F. K., Alsarra, I. A., Raish, M., Ansari, M. J., et al. (2020). Development of optimized clove oil nanoemulsion using Box–Behnken design: Characterization and evaluation for wound healing activity. *Journal of Drug Delivery Science and Technology, 55*, 101452. https://doi.org/10.1016/j.jddst.2019.101452
8. Mimica-Dukić, N., Božin, B., Soković, M., Mihajlović, B., & Matavulj, M. (2004). Antimicrobial and antioxidant activities of *Melissa officinalis* L. (Lamiaceae) essential oil. *Journal of Agricultural and Food Chemistry, 52*(9), 2485–2489. https://doi.org/10.1021/jf030698a
9. Ali, B., Al-Wabel, N. A., Shams, S., Ahamad, A., Khan, S. A., & Anwar, F. (2015). Essential oils used in aromatherapy: A systemic review. *Asian Pacific Journal of Tropical Biomedicine, 5*(8), 601–611. https://doi.org/10.1016/j.apjtb.2015.05.007
10. Ribeiro, L. N., Franz-Montan, M., Breitkreitz, M. C., de Paula, E., Groppo, F. C., Duarte, J. L., et al. (2012). Nanostructured lipid carriers versus nanoemulsions: Effects on lidocaine topical delivery. *Journal of Nanoparticle Research, 14*(11), 1–10.
11. Bouchemal, K., Briançon, S., Perrier, E., & Fessi, H. (2004). Nano-emulsion formulation using spontaneous emulsification: Solvent, oil and surfactant optimization. *International Journal of Pharmaceutics, 280*(1–2), 241–251. https://doi.org/10.1016/j.ijpharm.2004.05.016
12. Mishra, N., Tiwari, S., Verma, A., & Tiwari, G. (2013). UV spectrophotometric method development and validation of essential oil of *Eucalyptus globulus*. *Journal of Pharmaceutical Sciences and Bioscientific Research, 3*(1), 28–32.
13. Danaei, M., Dehghankhold, M., Ataei, S., Hasanzadeh Davarani, F., Javanmard, R., Dokhani, A., et al. (2018). Impact of particle size and polydispersity index on the clinical applications of lipidic nanocarrier systems. *Pharmaceutics, 10*(2), 57. https://doi.org/10.3390/pharmaceutics10020057
14. Shakeel, F., Haq, N., Alanazi, F. K., Alsarra, I. A., Ramadan, W., & Faiyazuddin, M. (2015). Formulation and optimization of nanoemulsions for topical delivery of hydrophobic drugs: Evaluation of physical stability and particle size. *Pharmaceutical Development and Technology, 20*(2), 188–196.
15. Gadkari, P. N., Patil, P. B., & Saudagar, R. B. (2019). Formulation, development and evaluation of topical nanoemulgel of tolnaftate. *Journal of Drug Delivery and Therapeutics, 9*, 208–213. https://doi.org/10.22270/jddt.v9i2-s.2495

 doi:10.20944/preprints202506.0615.v1

16. Choudhury, H., Gorain, B., Pandey, M., Chatterjee, L. A., Sengupta, P., Das, A., et al. (2017). Recent update on nanoemulgel as topical drug delivery system. *Journal of Pharmaceutical Sciences, 106*, 1736–1751. https://doi.org/10.1016/j.xphs.2017.03.042
17. Bashir, M., Ahmad, J., Asif, M., Khan, S. U., Irfan, M., & Ibrahim, A. Y. (2021). Nanoemulgel: An innovative carrier for diflunisal topical delivery with profound anti-inflammatory effect: In vitro and in vivo evaluation. *International Journal of Nanomedicine, 16*, 1457–1472. https://doi.org/10.2147/IJN.S294653
18. Oktay, A. N., Karakucuk, A., Ilbasmis Tamer, S., & Celebi, N. (2018). Dermal flurbiprofen nanosuspensions: Optimization with design of experiment approach and in vitro evaluation. *European Journal of Pharmaceutical Sciences, 122*, 254–263. https://doi.org/10.1016/j.ejps.2018.07.009
19. Mahmoud, R. A., Hussein, A. K., Nasef, G. A., & Mansour, H. F. (2020). Oxiconazole nitrate solid lipid nanoparticles: Formulation, in vitro characterization and clinical assessment of an analogous loaded carbopol gel. *Drug Development and Industrial Pharmacy, 46*(5), 706–716. https://doi.org/10.1080/03639045.2020.1752707
20. Clinical and Laboratory Standards Institute (CLSI). (2022). *Performance standards for antimicrobial susceptibility testing* (32nd ed., CLSI supplement M100). Wayne, PA: CLSI.
21. Wiegand, I., Hilpert, K., & Hancock, R. E. W. (2008). Agar and broth dilution methods to determine the minimal inhibitory concentration (MIC) of antimicrobial substances. *Nature Protocols, 3*(2), 163–175. https://doi.org/10.1038/nprot.2007.521
22. Shadab, M. D., Nabil, A. A., Aldawsari, H. M., Kotta, S., Ahmad, J., & Akhter, S. (2020). Improved analgesic and anti-inflammatory effect of diclofenac sodium by topical nanoemulgel: Formulation development, in vitro and in vivo studies. *Journal of Chemistry, 2020*, 1–10. https://doi.org/10.1155/2020/4071818
23. El-Leithy, E. S., Makky, A. M., Khattab, A. M., & Hussein, D. G. (2017). Nanoemulsion gel of nutraceutical co-enzyme Q10 as an alternative to conventional topical delivery system to enhance skin permeability and anti-wrinkle efficiency. *International Journal of Pharmacy and Pharmaceutical Sciences, 9*(10), 207–217. https://doi.org/10.22159/ijpps.2017v9i11.21751
24. Burki, I. K., Khan, M. K., Khan, B. A., Uzair, B., Braga, V. A., & Jamil, Q. A. (2020). Formulation development, characterization, and evaluation of a novel dexibuprofen-capsaicin skin emulgel with improved in vivo anti-inflammatory and analgesic effects. *AAPS PharmSciTech, 21*, 1–4. https://doi.org/10.1208/s12249-020-01760-7
25. Souto, E. B., & Müller, R. H. (2005). Transdermal delivery of ketoprofen using lecithin organogels: Mechanistic studies. *AAPS PharmSciTech, 6*(2), E237–E245. https://doi.org/10.1208/pt060234